How to cite: *Angew. Chem. Int. Ed.* **2021**, *60*, 1519–1523
International Edition: doi.org/10.1002/anie.202013480
German Edition: doi.org/10.1002/ange.202013480

Chalcogen Bonding

The Nature of Chalcogen-Bonding-Type Tellurium–Nitrogen Interactions: A First Experimental Structure from the Gas Phase

*Timo Glodde, Yury V. Vishnevskiy, Lars Zimmermann, Hans-Georg Stammler, Beate Neumann, and Norbert W. Mitzel**

Dedicated to Professor Thomas M. Klapötke on the occasion of his 60th birthday

Abstract: *$(C_6F_5)Te(CH_2)_3NMe_2$ (**1**), a perfluorophenyltellurium derivative capable of forming intramolecular N···Te interactions, was prepared and characterized. The donor-free reference substance $(C_6F_5)TeMe$ (**2**) and the unsupported adduct $(C_6F_5)(Me)Te{\cdot}NMe_2Et$ (**2 b**) were studied in parallel. Molecular structures of **1**, **2** and **2 b** were determined by single-crystal X-ray diffraction and for **1** and **2** by gas-phase electron diffraction. The structure of **1** shows N···Te distances of 2.639(1) Å (solid) and 2.92(3) Å (gas). Ab initio plus NBO and QTAIM calculations show significant charge transfer effects within the N···Te interactions and indicate σ-hole interactions.*

Dispersion interactions have recently received an increasing amount of attention.[1] They can add the decisive component in stabilizing otherwise weak interactions, for example, halogen bonding (XB) systems.[2] Hitherto, XB interactions were mainly studied by experiments in the solid or in solution phase.[3] However, under these conditions it is difficult to distinguish contributions to the strength of this interaction from intermolecular dispersion or electrostatic forces often summarized nonspecifically as "packing" or "solvent" effects.[4] The determination of quantitative energies and a qualitative interpretation of inter- and intramolecular interactions still remain challenging tasks.[1] There is also still a distinct paucity in corresponding gas-phase structure data because gas-phase experiments and data analyses are generally much more challenging and labor-intensive than those for the solid state.[5,6] The investigation of free molecules is, however, restricted in size, volatility and thermal stability of the compounds, and in particular difficult if weak interactions are involved due to soft-potential motions.

In 1990 Singh et al. reported the existence of special N···Te interactions in tellurium(IV) derivatives with benzylamine ligands in the solid phase.[7] The stabilizing effect was demonstrated by Hammerl et al. for the same benzylamine derivates[8] and Rakesh et al. crystallized a system containing N···Te–Cl units with a stronger interaction between nitrogen and tellurium atoms (2.355(3) Å in $ClTe(o\text{-}C_6H_4)\text{-}CH_2NMe_2$).[9] In fact, the investigated systems describe donating interactions between the heavy atom tellurium and the nitrogen atom, but a substantial proof in the gas phase is still missing to exclude pure solid-state effects.

For this purpose we now prepared (*N*,*N*-dimethylaminopropyl)(pentafluorophenyl)telluride (**1**) (Scheme 1). Its ^{125}Te-{^{1}H} NMR spectrum shows a triplet ($^3J_{Te,F} = 64$ Hz) at 353 ppm. The fact that the ^{125}Te{^{1}H} NMR resonance of $Te(C_6F_5)_2$ is a quintet at 305 ppm[10] allows to conclude the tellurium atom in **1** to be weakly coordinated in solution—intra- or intermolecularly—by an electronegative element such as nitrogen.

Suitable crystals for X-ray diffraction (XRD) of **1** were obtained by sublimation. Its molecular structure in the solid state (Figure 1) shows a N···Te distance of 2.639(1) Å. The distance from Te1 to the *ipso*-carbon atom C1 of the perfluorophenyl unit is 2.189(1) Å; this is rather long compared to bis(pentafluorophenyl)ditelluride at 2.124(1) Å[11] and bis(pentafluorophenyl)telluride[10] (2.101(6) Å) and is explicable by population of the antibonding Te1–C1 orbital by the donating nitrogen function in the NBO picture. As expected, the angle C1-Te1-C7 at 91.3(1)° is close to 90°. The angle C1-Te1···N1 at 166.4(1)° deviates slightly from the expected 180° for chalcogen bonding, likely due to ring restrictions.

The measured N···Te distance is more than one Å shorter than the sum of the van der Waals radii ($\Sigma r_{(vdW)} = 3.65$ Å).[12] The normalized contact distance, that is, the measured distance divided by the $\Sigma r_{(vdW)}$, at 0.72 describes the interaction more properly.

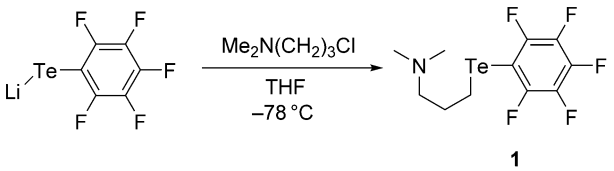

1

Scheme 1. Synthesis of compound **1**.

[*] T. Glodde, Dr. Y. V. Vishnevskiy, L. Zimmermann, Dr. H.-G. Stammler, B. Neumann, Prof. Dr. N. W. Mitzel
Universität Bielefeld, Fakultät für Chemie
Lehrstuhl für Anorganische Chemie und Strukturchemie
Universitätsstrasse 25, 33615 Bielefeld (Germany)
E-mail: mitzel@uni-bielefeld.de
Supporting information and the ORCID identification number(s) for the author(s) of this article can be found under: https://doi.org/10.1002/anie.202013480.

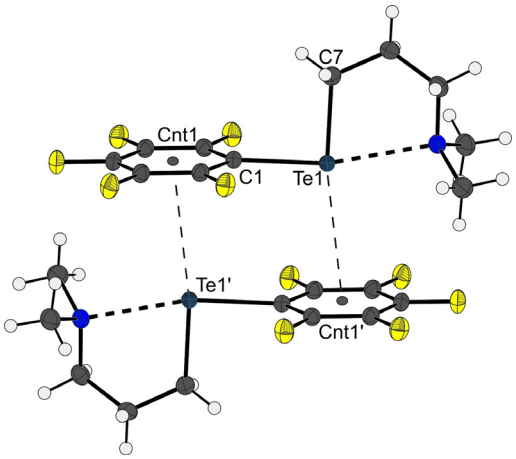

Figure 1. Molecular assembly of **1** in the crystal. The intermolecular Te1···C_6-ring centroid (Cnt′) distance of 3.662(1) Å and the C1-Te1-Cnt′ angle of 96.9(1)° indicate a dimerization by weak intermolecular interaction in the solid state. Symmetry code used for ′: $1-x,1-y,1-z$.

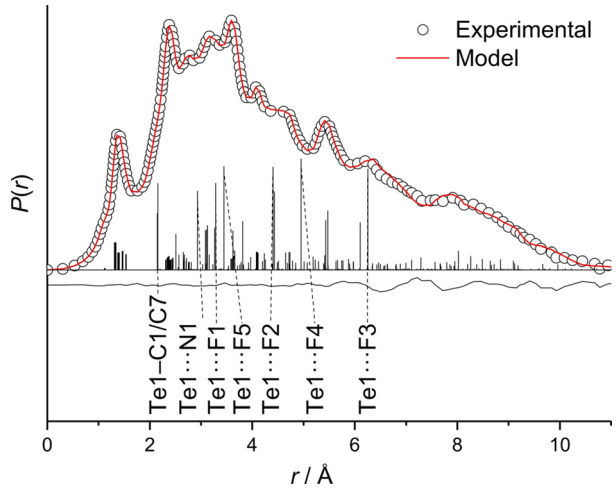

Figure 2. GED radial distribution curve of compound **1**. The circles represent experimental data, while the line represents the used model. The lower curve represents the difference curves between experiment and model.

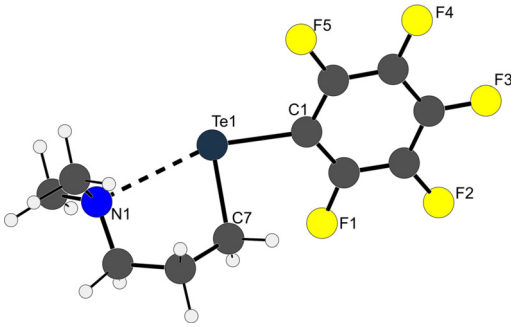

Figure 3. Gas-phase structure of **1** as determined by gas electron diffraction.

Since compound **1** is volatile and stable enough, we also performed a gas-phase electron-diffraction (GED) experiment in order to determine the distance between the nitrogen and tellurium atoms for the free molecule. The obtained GED data could be refined with a model that produced a sufficient fit described by an R_f factor of 4.0%. The GED analysis (Figure 2 and Figure 3) shows a single conformer to be sufficient to describe the data in the refinement properly.

In the gas phase, the N···Te distance refines to 2.92 Å with an error of 3σ of 0.03 Å (3σ errors are used throughout this article for GED parameters). The large standard deviation of the N···Te distance arises from the complex atomic electron scattering functions[13] of heavy atoms like Te. Haaland found this to result in an intrinsically low signal-to-background ratio during the analysis of $Te(CH_3)_2$.[14] The N···Te distance is longer than in the solid state (2.639(1) Å), but still shorter than $\Sigma r_{(vdW)}$, the normalized contact distance is 0.80 ± 0.02. This underlines the impact of a relatively strong non-covalent interaction. The fact that the weak N···Te bond is shorter in the solid than in the gas phase is in line with a significant donor–acceptor contribution as is frequently observed for datively bonded systems.[15,16] The weaker N···Te interaction in the gas phase is also consistent with a shorter Te1–C1 bond, due to a less pronounced donation into the antibonding Te1–C1 orbital (lp(N)→σ*(Te–C)).

The possibility of multiple conformers or dynamic systems in the gas phase has been explored, and any attempts to account for them do not lead to an improvement of the results.

The intramolecular angle C1-Te1···N1 is 161(2)°. This is in line with an interpretation in terms of an undistorted classical σ-hole interaction in the gas phase. Table 1 summarizes relevant structural parameters of compound **1** in the solid state and the gas phase as well as those calculated by DFT at two different levels. This allows to estimate the range of variation of theoretical data, even if comparatively similar methods are chosen.

The M06-2x[17] DFT level of theory was the starting point for investigations with the NBO and QTAIM concepts. The NBO analysis[18] found an n→σ* donation from N to Te associated to an NBO stabilization energy of 7.2 kcal mol^{-1}. The p-type orbital located at the Te atom donates electron density into the π system of the C_6F_5 unit leading to an NBO stabilization energy of 7.2 kcal mol^{-1}.

An analysis according to the Quantum Theory of Atoms in Molecules (QTAIM, Table 2) provides a small value for the charge density at the bond critical point (BCP) of the N···Te

Table 1: Summary of the most relevant structural parameters of compound **1**. The errors for the GED parameters are given as 3σ, for XRD 1σ. The parameter notation follows the crystallographic labels.

Phase	Method			
	XRD solid	GED (r_e) gas	PBE0-D3[a,c]	M06-2x[b,c]
d(Te1–C1) [Å]	2.189(1)	2.144(21)	2.150	2.076
d(Te1–C7) [Å]	2.159(1)	2.151(26)	2.159	2.112
d(N1···Te1) [Å]	2.639(1)	2.918(31)	2.751	2.899
α(N1···Te1-C1) [°]	166.4(1)	161(2)	165.8	162.9
α(C1-Te1-C7) [°]	91.3(1)	88.6(20)	92.0	92.2

[a] PBE0-D3/def2-TZVP. [b] M06-2x/def2-TZVPP. [c] single molecule.

Table 2: Selected intramolecular topological charge density parameters from the QTAIM analysis for compound **1**. Charge densities ρ [e Å^{-3}], Laplacian $\nabla^2\rho$ [e Å^{-5}], ellipticities ε (dimensionless) and bond path length BPL [Å].

	Bond	ρ(BCP)	$-\nabla^2\rho$(BCP)	ε	BPL
	Te1–C1	0.79	−5.18	0.19	2.040
1	Te1–C7	0.80	−1.34	0.18	2.076
	N1···Te1	0.17	−1.60	0.08	2.852

interaction of 0.17 e Å^{-3}. The corresponding Laplacian $-\nabla^2\rho$ (N,Te) has a very small negative value; this confirms that this interaction can be characterized as borderline between open and closed shell.[19] In contrast to these findings, earlier studies of comparable systems found no bond critical point between donor and acceptor atoms.[16]

To further explore these non-covalent interactions, we studied the nitrogen-free methyl(pentafluorophenyl)telluride (**2**) as a reference compound. Compound **2** was first described by Klein et al. but it was only characterized by its ^{19}F NMR spectrum and was then prepared from dimethyltellurium and iodopentafluorobenzene by irradiation with light.[20] We established a new synthesis for **2** using an alternative and rational approach: the reaction of lithium methyltelluride with bromopentafluorobenzene (Scheme 2).

The ^{1}H NMR spectrum of **2** shows a signal at 2.31 ppm while the ^{125}Te NMR spectrum of **2** shows a triplet of quartets at 210 ppm ($^{3}J_{\mathrm{Te,F}} = 32$ Hz), indicating the presence of a two-coordinate tellurium atom. The quartet results from a $^{2}J_{\mathrm{Te,H}}$ coupling to the three hydrogen atoms of the methyl group. The ^{13}C NMR spectrum of **2** reveals a triplet at −16 ppm with a $^{3}J_{\mathrm{F,C}}$ coupling constant of 4 Hz which is assigned to the methyl group. Furthermore, the signal related to the *ipso*-carbon atom shows a triplet of quartets at 84 ppm. The triplet arises from the $^{2}J_{\mathrm{F,C}}$ coupling with a coupling constant of 32 Hz and the quartett from a $^{3}J_{\mathrm{C,H}}$ coupling with the methyl group with a coupling constant of 4 Hz.

We were able to crystallize compound **2** using in situ crystallization techniques. The crystal structure of **2** (Figure 4) shows endless chains $(\mathbf{2})_{\infty}$ linked by Te···Te interactions (3.761(1) Å long), indicating the presence of chalcogen bonding. This is confirmed by the direction of the Te–C_{ipso} bond, which points, with angles of 164.8(1)° for C1-Te1···Te1′ and 122.4(1)° for C1-Te1···Te1″, onto the tellurium atoms of the neighboring molecules (crystallographically generated by two-fold screw axes). The Te1–C1 distance in solid **2** is 2.119(1) Å and the Te1–C7 distance is 2.137(2) Å.

The gas-phase structure of compound **2** was determined by GED (Figure 5). Table 3 summarizes selected important

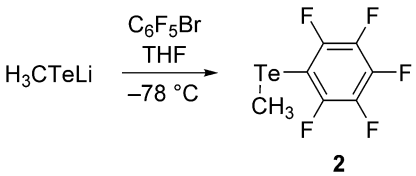

2

Scheme 2. Synthesis of **2**.

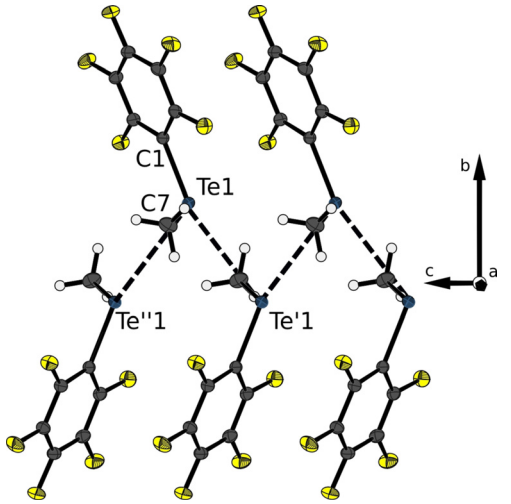

Figure 4. Molecular assembly of compound **2** in the solid state, view along the *a*-axis. Symmetry codes: ′ 1−*x*,−*y*,-1/2+*z*; ″ 1−*x*,−*y*,1/2+*z*.

structural parameters in comparison to solid state and theoretical values. The gas-phase data reveal a Te1–C1 distance of 2.077(16) Å, a Te1–C7 distance of 2.164(29) Å and a C1-Te1-C7 angle of 94(3)°. The problem of the complex scattering functions discussed above has an impact and results in large estimated standard deviations.

The obtained structural parameters for compound **2** show that the Te1–C7 distance is the same in the gaseous and solid phase within experimental error, whereas the Te1–C1 distance is shorter in the solid state. The latter results from the intermolecular Te···Te interaction in the crystal (see above), which is absent in the gas phase. Besides the different bond lengths, the angle C1-Te1-C7 is the same in gaseous and solid state within error ranges.

In order to compare this Te···Te-bonded with an—in contrast to **1**—unsupported N···Te-bonded situation and to

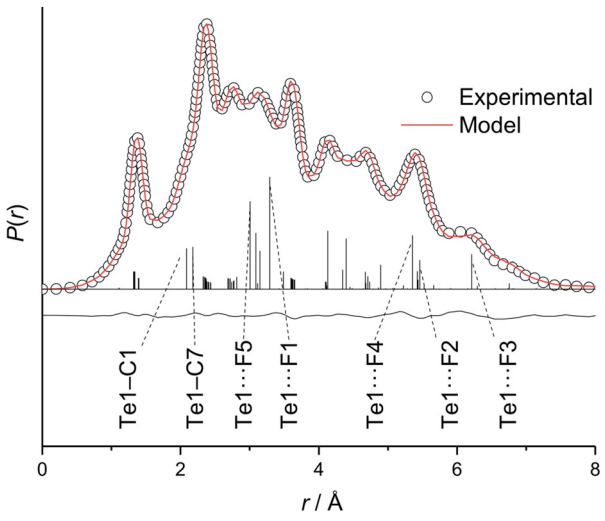

Figure 5. Experimental (dots) and model (line) radial distribution curves of **2**. The lower curve represents the difference curve (experiment-model).

Table 3: Summary of the most relevant structural parameters of compound **2**. The errors for the GED parameters are given as 3σ, for XRD 1σ.

Phase	Method			
	XRD solid	GED (r_e) gas	PBE0-D3[a,c]	M06-2x[b,c]
d(Te1–C1) [Å]	2.120(1)	2.077(16)	2.106	2.044
d(Te1–C7) [Å]	2.138(2)	2.164(29)	2.136	2.105
α(C1-Te1-C7) [°]	94.3(1)	94(3)	96.3	93.8

[a] PBE0-D3/def2-TZVP. [b] M06-2x/def2-TZVPP. [c] Single molecule.

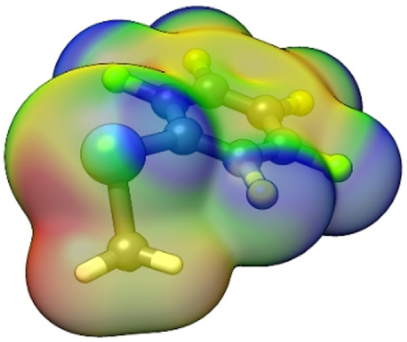

Figure 6. Electrostatic potential of **2** plotted onto an iso-electron-density surface of 0.001 eÅ^{-3} (M06-2x/def2-TZVPP). The red area indicates potential values of >20 kcal mol^{-1} (with a $V_{s,max}$ of 29 kcal mol^{-1}), the yellow area 5 to 20 kcal mol^{-1}, the green area -3 to 5 kcal mol^{-1} and blue <-3 kcal mol^{-1}.

describe the strength of a potential chalcogen bond better, a cocrystal of **2** with Me_2NEt was generated (complex **2b**) and examined by XRD. The unsupported N···Te contact measures 2.854(1) Å and the Te1–C1 distance is 2.160(1) Å (for more information see SI).

The availability of various chalcogen-bonding situations in compounds **2**, **2a** and **2b** provoked quantum-chemical studies to be performed on the relevant sections of the experimental crystal structures at the M06-2x/def2-TZVPP level (single molecules of **2**, a section of the $(\mathbf{2})_\infty$ chain: the dimer $(\mathbf{2})_2$ denoted **2a**, and complex **2b**; only H-atoms were optimized). The natural population analyses (NPA) show slightly smaller positive charge at the tellurium atom of **2** (0.54 e) compared to that in **1** (0.56 e). The most important contributions of the NBO analyses are donations of the nitrogen lone pair into the antibonding Te1−C1 orbital lp(N)→σ*(Te1−C1) (for **1**: 7.2, for **2b**: 9.1 kcal mol^{-1}) and a donation of the p-type lone pair located at the tellurium atom into the π system of the C_6F_5 unit, lp(Te, 5p)→π*(Te1−C1), for **1**, **2**, **2a** and **2b** (**1**: 7.2, **2**: 4.0, **2a**: 4.0, **2b**: 3.5 kcal mol^{-1}). The Quantum Theory of Atoms in Molecules (QTAIM, Table 4) provides the same small values for ρ at the BCPs of the Te···N bonds in **1** and **2b** (both 0.17 eÅ^{-3}) and an even smaller value for the Te···Te bond in **2a** (0.08 eÅ^{-3}). The Laplacian values $-\nabla^2\rho$ at these BCPs adopt small negative values (**1**: −1.6, **2b**: −1.4, **2a**: −0.8 eÅ^{-5}) indicating a depletion of electrons, compatible with more closed-shell-type, that is, dative interactions.

Using the WFA Surface Analysis Suite,[21] it was possible to determine the maximum of the electrostatic potential on the charge-density isosurface ($V_{s,max}$) of 29 kcal mol^{-1} for the isolated molecule **2** (Figure 6). It is located coaxially to the Te1−C1 bond and represents a σ-hole. Two of the observed local minima of the electrostatic potential on the charge-density isosurface ($V_{s,min}$) of compound **2** are located at the tellurium atom and indicate the positions of the lone pairs in an AX_2E_2 geometry (VSEPR model). These regions of $V_{s,min}$/$V_{s,max}$ at the calculated surface are comparable to the interacting regions in the molecular assembly in the solid state (Figure 4). This explains the crystallization behavior of **2**: each tellurium atom acts on one hand as a donor with its lone pair resulting in a C1-Te1-Te1″ angle of 122.4(1)° and on the other hand simultaneously with its σ-hole as acceptor resulting a C1-Te1-Te1′ angle of 164.8(1)°. This leads also to the conclusion that the surface potential of an isolated molecule **2** is high enough to interact with Lewis-basic regions (e.g. of amines), as was demonstrated with **1** and **2b**.

Table 4: Selected topological charge density parameters from the QTAIM analysis for compound **2a** and **2b**. Charge densities ρ [eÅ^{-3}], the Laplacian $-\nabla^2\rho$ [eÅ^{-5}], ellipticities ε (dimensionless) and bond path length BPL [Å].

	Bond	ρ(BCP)	$-\nabla^2\rho$(BCP)	ε	BPL
	C1−Te1	0.73	−3.80	0.17	2.120
2a	C7−Te1	0.74	−1.10	0.16	2.138
	Te1···Te1′	0.08	−0.75	0.15	3.776
	C1−Te1	0.69	−2.06	0.18	2.124
2b	C7−Te1	0.75	0.16	0.17	2.108
	N1···Te1	0.17	−1.40	0.24	2.808

The potential difference (ΔV_s) between **2** and dimethylethylamine (a model for the nitrogen-containing function in **1**) was calculated to be 60 kcal mol^{-1}, agreeing well with calculated electrostatic interactions (−94.7 kcal mol^{-1}) obtained by local energy decomposition analysis on DLPNO-CCSD(T)/def2-TZVPP[22] level of theory. Dispersion was shown in this context to have a minor contribution of the interaction energy by 1 % (for details see the Supporting Information, Table S8). This leads to the conclusion that **1** is predominantly stabilized by electrostatic interactions, which is in line with the QTAIM and NBO analysis. In essence, the quantum-chemical investigations showed that the obtained maximum of the electrostatic potential $V_{s,max}$ is a potentially stabilizing component of the weakly coordinated molecule **1**.

In summary, we herein present experimental and computational studies on tellurium compounds with a tendency to form adducts by chalcogen-type interactions. Compound **1** is the first example for an experimental study of a N···Te interaction in the gas phase. The N···Te distance in the gas at 2.918(31) Å is longer than in the solid state at 2.639(1) Å proving the presence of a significant dative component. Even though the molecule has the possibility of adopting several conformations, a sole conformer was found in both solid and gas phase, underlining the structurally determining importance of the interaction between N and Te atoms. The interactions can be explained by the electron-accepting behavior of the TeC_6F_5 unit. This was further confirmed

with $(C_6F_5)TeMe$ (**2**) showing an intermolecular Te···Te′ distance of 3.761(1) Å in the solid state. This fact is explicable by the simultaneously donating and accepting behavior of the Te atom, the latter is induced by the C_6F_5 group. Quantum-mechanical studies prove the interactions observed in **1** and **2** to arise from to the same origin.

Deposition numbers 2007089, 2007090 and 2022063 contain the supplementary crystallographic data for this paper. These data are provided free of charge by the joint Cambridge Crystallographic Data Centre and Fachinformationszentrum Karlsruhe Access Structures service.

Please note: Minor changes have been made to this manuscript since its publication as an Accepted Article. The Editor.

Acknowledgements

This work was funded by DFG (German Research Foundation) in the Priority Program SPP1807 "Control of LD in molecular chemistry", grant MI477/28-2, project no. 271386299), the core facility GED@BI (grant MI477/35-1, project no. 324757882), and a grant to Yu.V.V (VI 713/1–2, project no. 243500032). The authors gratefully acknowledge computing time provided by the Paderborn Center for Parallel computing (PC2). Open access funding enabled and organized by Projekt DEAL.

Keywords: chalcogen bonding · gas phase electron diffraction · intermolecular interactions · σ-holes

[1] J. P. Wagner, P. R. Schreiner, *Angew. Chem. Int. Ed.* **2015**, *54*, 12274 – 12296; *Angew. Chem.* **2015**, *127*, 12446 – 12471.
[2] a) P. Politzer, J. S. Murray, T. Clark, *Phys. Chem. Chem. Phys.* **2013**, *15*, 11178 – 11189; b) M. H. Kolář, P. Hobza, *Chem. Rev.* **2016**, *116*, 5155 – 5187.
[3] L. Vogel, P. Wonner, S. M. Huber, *Angew. Chem. Int. Ed.* **2019**, *58*, 1880 – 1891; *Angew. Chem.* **2019**, *131*, 1896 – 1907.
[4] a) P. C. Ho, P. Szydlowski, J. Sinclair, P. J. W. Elder, J. Kübel, C. Gendy, L. M. Lee, H. Jenkins, J. F. Britten, D. R. Morim, I. Vargas-Baca, *Nat. Commun.* **2016**, *7*, 11299; b) T. Caronna, R. Liantonio, T. A. Logothetis, P. Metrangolo, T. Pilati, G. Resnati, *J. Am. Chem. Soc.* **2004**, *126*, 4500 – 4501.
[5] H.-J. Schneider, *Angew. Chem. Int. Ed.* **2009**, *48*, 3924 – 3977; *Angew. Chem.* **2009**, *121*, 3982 – 4036.
[6] P. Metrangolo, G. Resnati, *Cryst. Growth Des.* **2012**, *12*, 5835 – 5838.
[7] H. B. Singh, N. Sudha, A. A. West, T. A. Hamor, *J. Chem. Soc. Dalton Trans.* **1990**, 907.
[8] A. Hammerl, T. M. Klapötke, B. Krumm, M. Scherr, *Z. Anorg. Allg. Chem.* **2007**, *633*, 1618 – 1626.
[9] P. Rakesh, H. B. Singh, R. J. Butcher, *Acta Crystallogr. Sect. E* **2012**, *68*, o214.
[10] T. M. Klapötke, B. Krumm, P. Mayer, K. Polborn, O. P. Ruscitti, *Inorg. Chem.* **2001**, *40*, 5169 – 5176.
[11] T. M. Klapötke, B. Krumm, P. Mayer, K. Polborn, O. P. Ruscitti, *J. Fluorine Chem.* **2001**, *112*, 207 – 212.
[12] S. Alvarez, *Dalton Trans.* **2013**, *42*, 8617 – 8636.
[13] T. C. Wong, L. S. Bartell, *J. Chem. Phys.* **1973**, *58*, 5654 – 5660.
[14] R. Blom, A. Haaland, R. Seip, R. Mäkelä, U. Kekäläinen, *Acta Chem. Scand.* **1983**, *37a*, 595 – 599.
[15] a) K. R. Leopold, M. Canagaratna, J. A. Phillips, *Acc. Chem. Res.* **1997**, *30*, 57 – 64; b) G. Forgács, M. Kolonits, I. Hargittai, *Struct. Chem.* **1990**, *1*, 245 – 250.
[16] a) N. W. Mitzel, K. Vojinović, R. Fröhlich, T. Foerster, H. E. Robertson, K. B. Borisenko, D. W. H. Rankin, *J. Am. Chem. Soc.* **2005**, *127*, 13705 – 13713; b) M. Hagemann, R. J. F. Berger, S. A. Hayes, H.-G. Stammler, N. W. Mitzel, *Chem. Eur. J.* **2008**, *14*, 11027 – 11038.
[17] a) Y. Zhao, D. G. Truhlar, *Theo. Chem. Acta* **2008**, *120*, 215 – 241; b) F. Weigend, R. Ahlrichs, *Phys. Chem. Chem. Phys.* **2005**, *7*, 3297 – 3305.
[18] A. E. Reed, R. B. Weinstock, F. Weinhold, *J. Chem. Phys.* **1985**, *83*, 735 – 746.
[19] R. F. W. Bader, *Chem. Rev.* **1991**, *91*, 893 – 928.
[20] D. Naumann, G. Klein, *Z. Anorg. Allg. Chem.* **1987**, *550*, 162 – 168.
[21] P. Politzer, K. E. Riley, F. A. Bulat, J. S. Murray, *Comput. Theor. Chem.* **2012**, *998*, 2 – 8.
[22] a) W. Schneider, G. Bistoni, M. Sparta, M. Saitow, C. Riplinger, A. A. Auer, F. Neese, *J. Chem. Theory Comput.* **2016**, *12*, 4778 – 4792; b) A. Altun, F. Neese, G. Bistoni, *J. Chem. Theory Comput.* **2019**, *15*, 215 – 228.

Manuscript received: October 6, 2020
Accepted manuscript online: October 22, 2020
Version of record online: November 17, 2020

